



Symposium of the International Society for Rock Mechanics

Temperature Induced Fracturing of Rock Salt Mass

Kurt Staudtmeister, Dirk Zapf*, Bastian Leuger, Marc Elend

Leibniz University of Hannover, IGtH/IUB, Welfengarten 1a, 30167 Hannover, Germany

Abstract

During the operation of gas storage caverns in rock salt mass the internal pressure changes during filling and withdrawal phases. Additionally temperature variations occur versus operation time. During withdrawal phases the temperature decreases which can lead to stress states in tensile regions at the cavern wall. Because the tensile strength of rock salt is relatively low compared to its compressive strength it is likely that tensile stresses lead to discrete fractures orthogonal to the direction of the tensile stresses.

If fractures of this kind are created – whether vertical or horizontal – the gas will penetrate into the fracture at the relevant pressure and further extend the length of the fractures under certain circumstances. There are currently no theoretical approaches describing the manner in which the fractures might propagate into the not by temperature changes influenced rock salt mass during repeated cyclic pressure changes. This aspect is topic of prospective research.

Salt caverns cannot be entered but only explored by sonar measurements, with which it is not possible to detect tensile fractures at the cavern wall. Within this paper examples from mining configurations will be shown where temperature changes lead to tensile fractures in the surrounding rock salt. These fractures have been well mapped while the temperature development is well documented.

The paper deals with recalculations under consideration of different salt properties of the temperature distributions and the resulting stress state in the surrounding rock salt mass. The stress calculation results and the consequences for the dimensioning of natural gas caverns are going to be discussed and assessed.

© 2017 The Authors. Published by Elsevier Ltd. This is an open access article under the CC BY-NC-ND license

(<http://creativecommons.org/licenses/by-nc-nd/4.0/>).

Peer-review under responsibility of the organizing committee of EUROCK 2017

Keywords: Rock mechanics; fracture propagation; gas storage; rock salt

* Corresponding author. Tel.: +495117622590; fax: +495117625367.

E-mail address: dirk.zapf@igth.uni-hannover.de

1. Introduction

The demands on the dimensioning of gas storage caverns in rock salt have changed considerably in recent years. The operating procedure of injection and withdrawal was influenced mostly seasonal. This meant a high gas inventory in the summer and therefore a high maximum internal cavern pressure, the gas withdrawal in autumn and winter and refilling the gas in the spring and summer, when gas was less needed [1, 2]. Within this phase relatively low operation rates were observed.

Nowadays from operators point of view it is required to have the greatest amount for the withdrawal and refill phase possible at any time of the year and at each pressure level of the cavern. This new target of operating a commercial gas cavern means a greater challenge for the geotechnical engineer regarding the dimensioning of the cavern.

The new operating modes include possibly more than a removal and filling in a year. Looking at the operation history of gas caverns in the last few decades, it is found that cavities have indeed experienced times with a pressure change rate of 10 bar/d or more. The question here is, however, how long was that period of withdrawal? Observing the average withdrawal rate of e.g. 30 days, it is found that the rate is only at 1-3 bar/d. This rate reflects the seasonal nature of the driven operating history of the existing gas caverns.

The new usage of caverns requires a higher rate over a withdrawal at any time. The task of the engineer is now to recommend pressure change rates on the economical and flexible side on the one hand without losing the stability and usability to endanger the cavern on the other hand [3-7]. Meanwhile, the dimensioning of gas caverns takes into account the change in temperature of the gas. These can cause rapid, significant changes in temperature during cyclic operations in the cavity. The difference between seasonal and cyclical storage has been shown in [8].

Rock salt has a low tensile strength with values in the bandwidth of 0.0-2.0 MPa. Because strong cooling due to the thermodynamic processes in gas at withdrawals could occur, it is likely that these temperature changes may lead to stress states in tensile regions at the cavern wall. The question is whether these stresses can lead to macroscopic fractures and thus the stability and tightness can compromise the cavern due to a penetration of gas under high pressure into the open fracture.

Since the gas caverns in rock salt are not accessible, it is extremely difficult to prove whether the thermally induced stress states on the cavern wall lead to macroscopic fractures. A sonar survey cannot detect fractures in radial or vertical direction because radial distances of the cavern walls remain unchanged. Likewise, in storage mode, a significant loss of gas cannot be recorded immediately.

In Germany, there are examples where macroscopic fractures due to temperature changes have been observed in rock salt. On the one hand this is a field test for the storage of LNG [9] and the other hand the observation of macroscopic fractures in a shaft of a rock salt mine in Gorleben [10].

The aim of this paper is to present numerical calculations carried out for the latter example, with an outlook on the consequences for storage of natural gas and to show future research requirements in the field of fracture modelling.

2. In situ examples

2.1. Studies on the Storage of LNG in Salt Cavities

In the Kyrogas field test Hansa (Empelde) a test cavern with a volume of app. 2 m³ was leached in a salt mine and went through an extensive testing program. These tests were carried out with liquid nitrogen. The cavern was produced at a depth of about 600 m [9].

During the test, liquid nitrogen was filled into the cavern over a period of 52 hours. Besides the recording of the noises in the cavern with a geophone the cavern wall was observed through a Plexiglas window. The temperature dropped after a day at the cavern wall to a value of about 76 K (compared to the primary rock temperature of about 300 K).

The geophone recorded immediately after filling the liquid nitrogen the loudest noises as an indicator for cracking of the rock salt. Through the Plexiglas cover vertical fractures could be observed with opening

widths of 1-2 mm. They joined again when the temperature of the liquid nitrogen in the cavern began to rise because of the heat flow from the surrounding rock mass.

It should be noted that due to the sudden and very strong temperature change in the test cavern macroscopic fractures occur on the wall. Questions that appeared in connection with the storage of LNG in rock salt caverns were the following:

Will the fractures be arrested at a certain distance from the cavity wall? Will the cavity be stable in spite of the fracture formation?

These questions were also discussed in several gas cavern projects [4, 11].

2.2. Thermal induced fractures in the Gorleben shaft

The temperature difference in the previous example was very large. Therefore, the comparison with the temperature cooling in a gas cavern is not necessarily given. This field test should demonstrate that fractures may occur due to temperature change in the rock salt.

With the observations in the shaft Gorleben [10] another example is available, which is located with respect to the measured temperature differences closer to the range of temperature changes in a gas cavern.

In this example, between two shafts of the Gorleben exploration mine ventilation system was built from shaft 1 to shaft 2. Due to the connection, there was an air circulation, which led with seasonal fluctuations of the ventilation temperature to a difference in the shaft 1 of up to 20 K.

Because of these temperature changes on the shaft 1 fractures were detected. Figure 1 shows an exploration of the horizon of the geological survey of the ventilation-induced fractures at a depth of about 370-380 m. More photos of later years indicate that the fractures have closed again due to more favourable mine ventilation. Noticeable in this connection is that the opening widths of the fractures are in upper horizons larger than in greater depth of the shaft. Heusermann and Eickemeier (BGR) [10] have carried first tests of numerical studies to demonstrate that the observed macro-fractures caused by the temperature cooling out.

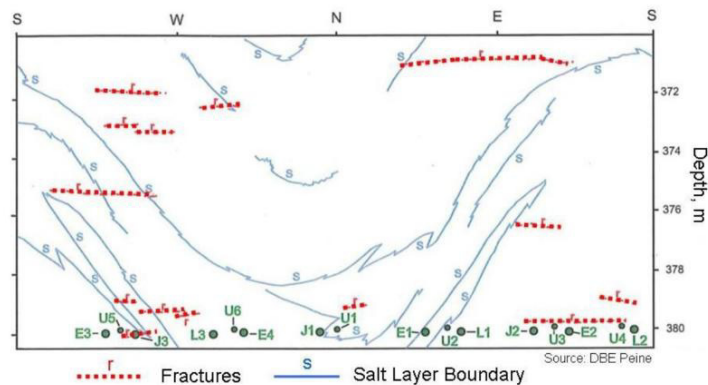


Fig. 1. Mapping of fractures at the shaft wall in Gorleben.

This example has now been investigated in this paper again numerically. It will give a first indication of the effect on the cyclic operation mode and the future research work aimed at the fracture progression.

3. Calculations

3.1. Shaft Gorleben: Geometry and initial values

The shaft model for the calculations includes a cylindrical quarter model. The radius is 3.75 m and the discretization size at the shaft wall is set at 20 cm in the radial direction. The distance between the outer edges from the shaft axis is 200 m and the model height is set at 50 m. Figure 2 shows the structure of the calculation model.

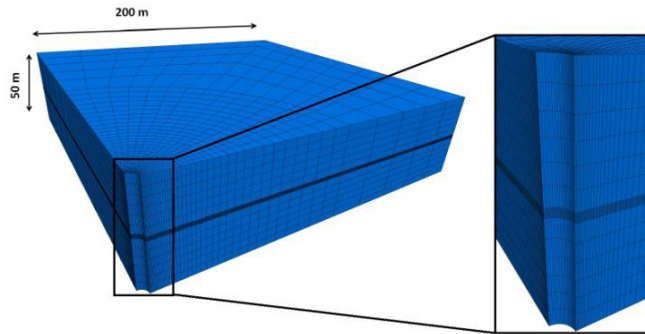


Fig. 2. Geometry and discretization of the shaft model.

The depth of the generated model ranges from 545 m to 595 m. In the middle of the model there is a homogenous and isotropic primary stress state of about -12.5 MPa. The primary rock mass temperature is estimated at 305 K with respect to the center of the calculation model. The calculation model contains 16,875 zones and 19,136 grid points. For the rock salt the time dependent constitutive law Lubby2 is used. Table 1 shows the elastic and viscous parameters used for the calculations.

Table 1. Rock salt mass material properties.

| Parameter | Value |
|-------------------------------|---|
| Young's Modulus E | 18000 – 25000 MPa |
| Poisson's ratio ν | 0.25 – 0.35 |
| Maxwell viscosity η_m^* | $7 \cdot 10^{13}$ |
| m | -0.39 MPa^{-1} |
| l | -0.05 K^{-1} |
| Kelvins shear modulus G_k^* | $5.5 \cdot 10^3 \text{ MPa}$ |
| k_1 | -0.1 MPa^{-1} |
| Kelvin viscosity η_k^* | $4.3 \cdot 10^3 \text{ d} \cdot \text{MPa}$ |
| k_2 | -0.05 MPa^{-1} |

For the thermo-mechanical coupled calculations, the following thermal properties in Table 2 for the rock salt have been applied.

Table 2. Rock salt mass properties for the thermal calculation.

| Parameter | Value |
|-----------------------------|---|
| Young's Modulus E | 18000 – 25000 MPa |
| Kelvin viscosity η_k^* | $4.3 \cdot 10^3 \text{ d} \cdot \text{MPa}$ |
| k_2 | -0.05 MPa^{-1} |

3.2. Shaft Gorleben: temperature evolution

The Gorleben shaft 1 showed due to the ventilation a temperature difference of about 20 K. This temperature difference over a period of 80 days is applied after a time period of one year on a constant temperature level to the shaft wall in the model. The time profile of temperature evolution is shown in Figure 3.

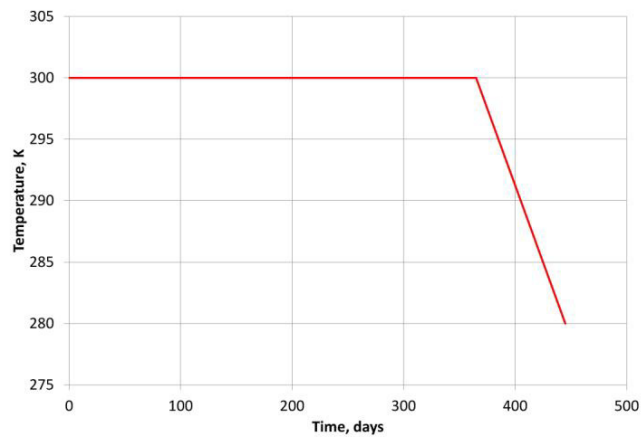


Fig. 3. Temperature loading history.

3.3. Calculation 1: model without fracture propagation

The first model is calculated with the temperature distribution from section 3.2. The stress state is going to be evaluated in the middle of the calculation model.

The temperature in the shaft was estimated at 300 K and recognizable influences the distribution of the rock salt mass temperature ($T = 305$ K). The stress components of rock salt influenced by the creep behaviour are developing as expected. A control is the value of the radial stress component σ_r at the shaft wall which must be equal to the internal pressure. Since the shaft is under atmospheric pressure, the radial stress component σ_r takes on the value 0 MPa. Also to be noticed is that the model dimension was chosen with 200 m in horizontal direction sufficiently large, because the stress components reach the primary stress state of -12.5 MPa.

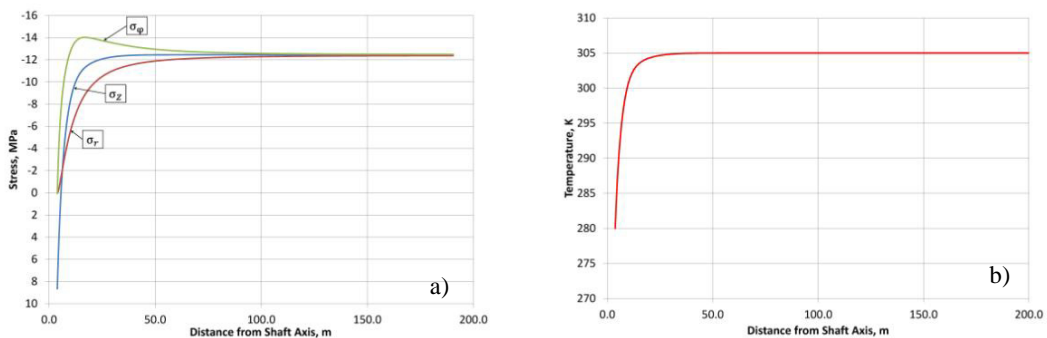


Fig. 4. a) Principal stresses after temperature decrease; b) temperature distribution after 80 days of cooling.

After the subsequent temperature decrease to $T = 280 \text{ K}$ (Figure 4b) over 80 days the stress state is distributed as shown in Figure 4a. It is shown that the vertical stress component σ_z shows values in a significant stress region around 8.6 MPa. The circumferential stress σ_θ has approached a range near the tensile stress boundary. Overall a tensile stress zone with a horizontal expansion from the shaft wall into the rock mass can be detected with app. 1.6 m.

From engineering point of view even raises the question: Are these calculated stress conditions realistic?

It is known from laboratory testings that rock salt only has a very low tensile strength of about 0.0-2.0 MPa. In the example considered, the salt would be fractured by calculation already long before the end of the 80-day temperature drop. At this point, at least theoretically the observed evidence of tension fractures is carried out at the Gorleben shaft. With the scheduled parameters and the temperature load case can be concluded that the fractures occurred due to the temperature drop.

But, as a fractured system cannot taken up further tensile stresses, the model has to be modified and recalculated.

3.4. Calculation 2: model with fracture propagation

Figure 5 shows the proximity of the calculation model with the fine discretized midsection. Here, fracture elements are taken into account, which according to the exceeding of a defined ultimate tensile strength σ_t^u , are going to be deleted from the system successively. This assumption is based on research of fracture propagation in concrete [12, 13], where fracturing begins to exceed the tensile strength. The temperature load case is identical to calculation example 1.

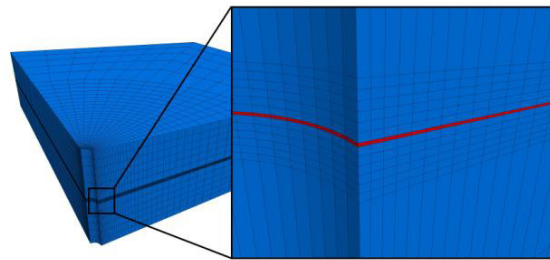


Fig. 5. Geometry and discretization of the modified shaft model (red zones show fracture elements).

Figure 6a shows the calculation model at $t = 445$ days after the cooling of the shaft at $T = 20 \text{ K}$. Clearly visible here is that the fracture elements were taken out of the system during the calculation.

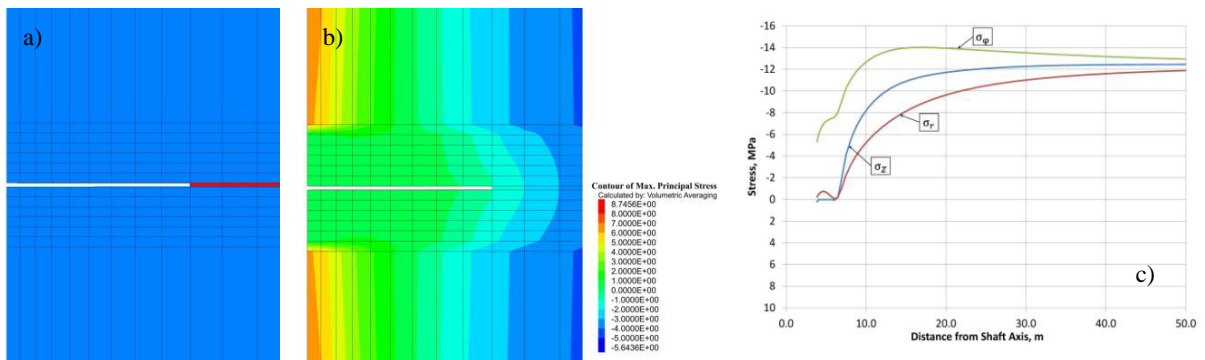


Fig. 6. a) Fracture elements after 80 days cooling; b) maximum stress distribution; c) principal stresses after cooling above fracture.

The distribution of the maximum principal stress component around the fracture is shown in figure 6b , while the stress distribution of the three main stresses in a section above the fracture elements (distance 12 cm) is shown in Figure 6c. Comparing now the stress state with the stress state calculated at a continuum model without fracture propagation (Figure 4a), following facts can be observed:

- The vertical stress component σ_z does not reach the tensile stress.
- The circumferential stress component σ_ϕ remains clearly in the compression stress.
- After about 5 m distance from the shaft wall the stress states in the continuum and discontinuum model are almost identical.
- The propagation of the fracture is approximately 2.90 m and is therefore about 1.30 m longer than the calculated tensile stress zone in example 1.

4. Assessment of the results

The stress distribution around the fracture simulated in this example is significant different from that off an undisturbed continuum system. For that it can be noted from the comparison that it is not possible to calculate and assess the stress state of a system with a continuum model in which a fracture should occur computationally due to the appearance of tensile stresses.

If the development of fractures is to be taken into account in the system, then it is necessary to include a proper formulation in the calculations.

The model calculation in example 2 within the framework of this paper is only the beginning of a series of studies in the future.

A major challenge is to recalculate the distribution of fractures in the shaft Gorleben realistically. At the moment the computational model can only delete zones with special properties. Looking at the vertical stresses on the overall height at the shaft wall in the model, it is visible that tensile stresses occur in about 2 meters distance from the fracture elements. The next modification of the calculation model would be a further refinement of the fracture elements. However, this leads of course to longer computing times.

Another step in this analysis is the consideration of an internal pressure, as it also prevails in a gas cavern. In example 2 the shaft is calculated as mentioned with atmospheric pressure. If a fracture in a cavern filled with gas would occur, gas would immediately shoot into the open fracture with a corresponding pressure. The question of whether and where the fracture ends in the rock salt is part of future research.

5. Conclusions

The paper gives an indication of the prevalent stress state in a disturbed system with a progressive fracture. In the presented model, there is need for further developments, which are clearly the discretization of further fractures in the elements and the consideration of an internal pressure at a cavern wall and finally in the fracture itself.

It is very likely that a fracture is finite behind a cavern wall, because the primary rock mass stresses are large enough at a certain distance from the cavern to stop the fracture progression. If there are any fractures in a cavern wall (due to irregular shapes, this is likely), this may not lead to immediate loss of stability and tightness of the cavern.

The design of a gas cavern always refers to the envelope of an actual cavern form. While research has not provided proof that fractures are at some distance from the cavity wall finite, it is recommended to avoid tensile stresses when dimensioning the gas withdrawal rate for high cycling storage.

References

- [1] K. Staudtmeister, D. Struck, Design Criteria for Prevention of Creep Rupture for Gas Caverns in Salt Rock Mass, SMRI Fall Meeting, Paris, 1990.
- [2] R.B. Rokahr, K. Staudtmeister, D. Zander-Schiebenhöfer, Rock Mechanical Determination of the Maximum Internal Pressure for Gas Storage Caverns in Rock Salt, SMRI Fall Meeting, Rome, 1998.
- [3] R.B. Rokahr, K. Staudtmeister, D. Zapf, Influence of Different Loading Histories on the Rock Mechanical Behavior of a Gas Cavern at Shallow Depth, SMRI Spring Meeting, Porto, 2008.
- [4] R.B. Rokahr, K. Staudtmeister, D. Zapf, Rock Mechanical Design for a Planned Gas Cavern Field in the Preesall Project Area, Lancashire, UK, SMRI Fall Meeting, York, 2011.
- [5] S. Yildirim, D. Zapf, K. Staudtmeister, Rock mechanical design of gas storage caverns, Eurock 2016, Cappadocia, Turkey.
- [6] K. Staudtmeister, D. Zapf, Rock Mechanical Design of Gas Storage Caverns in Rock Salt Mass with Cyclic Operations, 13th International Congress on Rock Mechanics 2015, Montréal, Canada.
- [7] K. Staudtmeister, D. Zapf, B. Leuger, The Influence of Different Loading Scenarios on the Thermo – Mechanical Behavior of a Gas Storage Cavern, SMRI Spring Meeting, Galveston, 2011.
- [8] K. Staudtmeister, D. Zapf, Rock Mechanical Design of Gas Storage Caverns for Seasonal Storage and Cyclic Operations, SMRI Spring Meeting, Grand Junction, 2010.
- [9] H.G. Haddenhorst, H. Lorenzen, K. Schwier, Studies on the Storage of LNG in Salt Caverns“, in: 5th I. Conf. Liquefied Nat. Gas, Inst. Gas Tech. II, 8., Chicago, 1977.
- [10] S. Heusermann, R. Eickemeier, Influence of the ventilation temperature on the mechanical behavior of shaft 1 in the Gorleben Exploration Mountain (in German), Messen in der Geotechnik 2008, Facheminar 23rd/24th October 2008, Braunschweig.
- [11] C. Pellizzaro, G. Bergeret, A. Leadbetter, Y. Charnavel, Thermo-Mechanical behavior of Stublach gas storage caverns, SMRI Fall Meeting, York, 2011.
- [12] C. Kessler-Kramer, Tensile behavior of concrete under fatigue stress (in German), Karlsruhe, 2002.
- [13] A. Hillerborg, M. Modéer, P. E. Petersson, Analysis of Crack Formation and Crack Growth in Concrete by Means of Fracture Mechanics and Finite Elements, Cement Concrete Res. 6 (1976).